EUROPEAN ORGANIZATION FOR NUCLEAR RESEARCH

CERN-PPE/95-019
22 February 1995

Improved measurements of the B^0 and B^+ meson lifetimes

The OPAL Collaboration

Abstract

Updated measurements of the B^0 and B^+ meson lifetimes are presented. From a data sample of 1.72 million hadronic Z^0 decays recorded during the period 1991 to 1993, a sample of approximately 1000 semileptonic B meson decays containing a D^0, D^+ or D^{*+} has been isolated. From the distribution of decay times in the different samples the lifetimes of the B^0 and B^+ mesons are determined to be $1.53 \pm 0.12 \pm 0.08$ ps and $1.52 \pm 0.14 \pm 0.09$ ps, respectively, where the first error is statistical and the second systematic. The ratio of the B^+ to B^0 lifetimes is measured to be $0.99 \pm 0.14^{+0.05}_{-0.04}$, confirming expectations that the lifetimes are similar.

(To be submitted to Zeitschrift für Physik C.)

The OPAL Collaboration

R. Akers[16], G. Alexander[23], J. Allison[16], K. Ametewee[25], K.J. Anderson[9], S. Arcelli[2], S. Asai[24], D. Axen[29], G. Azuelos[18,a], A.H. Ball[17], E. Barberio[26], R.J. Barlow[16], R. Bartoldus[3], J.R. Batley[5], G. Beaudoin[18], A. Beck[23], G.A. Beck[13], C. Beeston[16], T. Behnke[27], K.W. Bell[20], G. Bella[23], S. Bentvelsen[8], P. Berlich[10], S. Bethke[14], O. Biebel[14], I.J. Bloodworth[1], P. Bock[11], H.M. Bosch[11], M. Boutemeur[18], S. Braibant[12], P. Bright-Thomas[25], R.M. Brown[20], A. Buijs[8], H.J. Burckhart[8], R. Bürgin[10], C. Burgard[27], N. Capdevielle[18], P. Capiluppi[2], R.K. Carnegie[6], A.A. Carter[13], J.R. Carter[5], C.Y. Chang[17], C. Charlesworth[6], D.G. Charlton[1,b], S.L. Chu[4], P.E.L. Clarke[15], J.C. Clayton[1], S.G. Clowes[16], I. Cohen[23], J.E. Conboy[15], O.C. Cooke[16], M. Cuffiani[2], S. Dado[22], C. Dallapiccola[17], G.M. Dallavalle[2], C. Darling[31], S. De Jong[12], L.A. del Pozo[8], H. Deng[17], M. Dittmar[4], M.S. Dixit[7], E. do Couto e Silva[12], J.E. Duboscq[8], E. Duchovni[26], G. Duckeck[8], I.P. Duerdoth[16], U.C. Dunwoody[5], J.E.G. Edwards[16], P.A. Elcombe[5], P.G. Estabrooks[6], E. Etzion[23], H.G. Evans[9], F. Fabbri[2], B. Fabbro[21], M. Fanti[2], P. Fath[11], M. Fierro[2], M. Fincke-Keeler[28], H.M. Fischer[3], P. Fischer[3], R. Folman[26], D.G. Fong[17], M. Foucher[17], H. Fukui[24], A. Fürtjes[8], P. Gagnon[6], A. Gaidot[21], J.W. Gary[4], J. Gascon[18], N.I. Geddes[20], C. Geich-Gimbel[3], S.W. Gensler[9], F.X. Gentit[21], T. Geralis[20], G. Giacomelli[2], P. Giacomelli[4], R. Giacomelli[2], V. Gibson[5], W.R. Gibson[13], J.D. Gillies[20], J. Goldberg[22], D.M. Gingrich[30,a], M.J. Goodrick[5], W. Gorn[4], C. Grandi[2], E. Gross[26], J. Hagemann[27], G.G. Hanson[12], M. Hansroul[8], C.K. Hargrove[7], P.A. Hart[9], M. Hauschild[8], C.M. Hawkes[8], E. Heflin[4], R.J. Hemingway[6], G. Herten[10], R.D. Heuer[8], J.C. Hill[5], S.J. Hillier[8], T. Hilse[10], P.R. Hobson[25], D. Hochman[26], R.J. Homer[1], A.K. Honma[28,a], R. Howard[29], R.E. Hughes-Jones[16], P. Igo-Kemenes[11], D.C. Imrie[25], A. Jawahery[17], P.W. Jeffreys[20], H. Jeremie[18], M. Jimack[1], M. Jones[6], R.W.L. Jones[8], P. Jovanovic[1], C. Jui[4], D. Karlen[6], J. Kanzaki[24], K. Kawagoe[24], T. Kawamoto[24], R.K. Keeler[28], R.G. Kellogg[17], B.W. Kennedy[20], B. King[8], J. King[13], J. Kirk[29], S. Kluth[5], T. Kobayashi[24], M. Kobel[10], D.S. Koetke[6], T.P. Kokott[3], S. Komamiya[24], R. Kowalewski[8], T. Kress[11], P. Krieger[6], J. von Krogh[11], P. Kyberd[13], G.D. Lafferty[16], H. Lafoux[8], R. Lahmann[17], W.P. Lai[19], J. Lauber[8], J.G. Layter[4], P. Leblanc[18], A.M. Lee[31], E. Lefebvre[18], D. Lellouch[26], C. Leroy[18], J. Letts[2], L. Levinson[26], S.L. Lloyd[13], F.K. Loebinger[16], G.D. Long[17], B. Lorazo[18], M.J. Losty[7], X.C. Lou[8], J. Ludwig[10], A. Luig[10], M. Mannelli[8], S. Marcellini[2], C. Markus[3], A.J. Martin[13], J.P. Martin[18], T. Mashimo[24], W. Matthews[25], P. Mättig[3], U. Maur[3], J. McKenna[29], T.J. McMahon[1], A.I. McNab[13], F. Meijers[8], F.S. Merritt[9], H. Mes[7], A. Michelini[8], R.P. Middleton[20], G. Mikenberg[26], D.J. Miller[15], R. Mir[26], W. Mohr[10], A. Montanari[2], T. Mori[24], M. Morii[24], U. Müller[3], B. Nellen[3], B. Nijjhar[16], S.W. O'Neale[1], F.G. Oakham[7], F. Odorici[2], H.O. Ogren[12], N.J. Oldershaw[16], C.J. Oram[28,a], M.J. Oreglia[9], S. Orito[24], F. Palmonari[2], J.P. Pansart[21], G.N. Patrick[20], M.J. Pearce[1], P.D. Phillips[16], J.E. Pilcher[9], J. Pinfold[30], D.E. Plane[8], P. Poffenberger[28], B. Poli[2], A. Posthaus[3], T.W. Pritchard[13], H. Przysiezniak[30], M.W. Redmond[8], D.L. Rees[8], D. Rigby[1], M.G. Rison[5], S.A. Robins[13], D. Robinson[5], N. Rodning[30], J.M. Roney[28], E. Ros[8], A.M. Rossi[2], M. Rosvick[28], P. Routenburg[30], Y. Rozen[8], K. Runge[10], O. Runolfsson[8], D.R. Rust[12], M. Sasaki[24], C. Sbarra[2], A.D. Schaile[8], O. Schaile[10], F. Scharf[3], P. Scharff-Hansen[8], P. Schenk[4], B. Schmitt[3], M. Schröder[8], H.C. Schultz-Coulon[10], P. Schütz[3], M. Schulz[8], C. Schwick[27], J. Schwiening[3], W.G. Scott[20], M. Settles[12], T.G. Shears[5], B.C. Shen[4], C.H. Shepherd-Themistocleous[7], P. Sherwood[15], G.P. Siroli[2], A. Skillman[15], A. Skuja[17], A.M. Smith[8], T.J. Smith[28], G.A. Snow[17], R. Sobie[28], S. Söldner-Rembold[10], R.W. Springer[30], M. Sproston[20], A. Stahl[3], M. Starks[12], C. Stegmann[10], K. Stephens[16],

J. Steuerer[28], B. Stockhausen[3], D. Strom[19], P. Szymanski[20], R. Tafirout[18], H. Takeda[24], T. Takeshita[24], P. Taras[18], S. Tarem[26], M. Tecchio[9], P. Teixeira-Dias[11], N. Tesch[3], M.A. Thomson[8], O. Tousignant[18], S. Towers[6], M. Tscheulin[10], T. Tsukamoto[24], A.S. Turcot[9], M.F. Turner-Watson[8], P. Utzat[11], R. Van Kooten[12], G. Vasseur[21], P. Vikas[18], M. Vincter[28], A. Wagner[27], D.L. Wagner[9], C.P. Ward[5], D.R. Ward[5], J.J. Ward[15], P.M. Watkins[1], A.T. Watson[1], N.K. Watson[7], P. Weber[6], P.S. Wells[8], N. Wermes[3], B. Wilkens[10], G.W. Wilson[27], J.A. Wilson[1], V-H. Winterer[10], T. Wlodek[26], G. Wolf[26], S. Wotton[11], T.R. Wyatt[16], A. Yeaman[13], G. Yekutieli[26], M. Yurko[18], V. Zacek[18], W. Zeuner[8], G.T. Zorn[17].

[1]School of Physics and Space Research, University of Birmingham, Birmingham B15 2TT, UK
[2]Dipartimento di Fisica dell' Università di Bologna and INFN, I-40126 Bologna, Italy
[3]Physikalisches Institut, Universität Bonn, D-53115 Bonn, Germany
[4]Department of Physics, University of California, Riverside CA 92521, USA
[5]Cavendish Laboratory, Cambridge CB3 0HE, UK
[6]Carleton University, Department of Physics, Colonel By Drive, Ottawa, Ontario K1S 5B6, Canada
[7]Centre for Research in Particle Physics, Carleton University, Ottawa, Ontario K1S 5B6, Canada
[8]CERN, European Organisation for Particle Physics, CH-1211 Geneva 23, Switzerland
[9]Enrico Fermi Institute and Department of Physics, University of Chicago, Chicago IL 60637, USA
[10]Fakultät für Physik, Albert Ludwigs Universität, D-79104 Freiburg, Germany
[11]Physikalisches Institut, Universität Heidelberg, D-69120 Heidelberg, Germany
[12]Indiana University, Department of Physics, Swain Hall West 117, Bloomington IN 47405, USA
[13]Queen Mary and Westfield College, University of London, London E1 4NS, UK
[14]Technische Hochschule Aachen, III Physikalisches Institut, Sommerfeldstrasse 26-28, D-52056 Aachen, Germany
[15]University College London, London WC1E 6BT, UK
[16]Department of Physics, Schuster Laboratory, The University, Manchester M13 9PL, UK
[17]Department of Physics, University of Maryland, College Park, MD 20742, USA
[18]Laboratoire de Physique Nucléaire, Université de Montréal, Montréal, Quebec H3C 3J7, Canada
[19]University of Oregon, Department of Physics, Eugene OR 97403, USA
[20]Rutherford Appleton Laboratory, Chilton, Didcot, Oxfordshire OX11 0QX, UK
[21]CEA, DAPNIA/SPP, CE-Saclay, F-91191 Gif-sur-Yvette, France
[22]Department of Physics, Technion-Israel Institute of Technology, Haifa 32000, Israel
[23]Department of Physics and Astronomy, Tel Aviv University, Tel Aviv 69978, Israel
[24]International Centre for Elementary Particle Physics and Department of Physics, University of Tokyo, Tokyo 113, and Kobe University, Kobe 657, Japan
[25]Brunel University, Uxbridge, Middlesex UB8 3PH, UK
[26]Particle Physics Department, Weizmann Institute of Science, Rehovot 76100, Israel
[27]Universität Hamburg/DESY, II Institut für Experimental Physik, Notkestrasse 85, D-22607 Hamburg, Germany
[28]University of Victoria, Department of Physics, P O Box 3055, Victoria BC V8W 3P6, Canada
[29]University of British Columbia, Department of Physics, Vancouver BC V6T 1Z1, Canada

[30]University of Alberta, Department of Physics, Edmonton AB T6G 2J1, Canada
[31]Duke University, Dept of Physics, Durham, NC 27708-0305, USA

[a]Also at TRIUMF, Vancouver, Canada V6T 2A3
[b] Royal Society University Research Fellow

1 Introduction

The comparison of the lifetimes of different species of weakly decaying b hadrons provides a direct test of the validity of the spectator model. Variations in lifetime due to non-spectator processes may be expected to occur at the 10% level [1]. Measurements of the average[1] b hadron lifetime with data from the LEP experiments [2] are insensitive to such variations. However, the b hadron lifetimes are required to determine the Cabbibo-Kobayashi-Maskawa matrix element V_{cb}, which governs the b quark coupling to the c quark. Certain methods of determining V_{cb} rely on the use of a specific b hadron lifetime [3], so the use of an average lifetime would be incorrect. It is therefore of interest to measure the lifetimes of the different b hadron species. These can be separated by reconstructing b hadrons in (semi-)exclusive decay modes.

We have previously presented measurements [4] of the B^0 and B^+ meson lifetimes using data recorded by OPAL in 1991. Other measurements of individual b hadron lifetimes have been made elsewhere [5, 6, 7, 8].

B^0 and B^+ mesons are tagged using semileptonic decays with a reconstructed charm meson:

$$B \to \overline{D}^0 \ell^+ X, \qquad B \to D^- \ell^+ X, \qquad B \to D^{*-} \ell^+ X,$$

where ℓ is either an electron or a muon, and X denotes additional particles which include the neutrino. Charge conjugation is implicitly assumed throughout this paper, and the symbol $D^{(*)}$ is used to denote either a D or D^* meson. These decay modes allow partial separation of B^+ and B^0. We reconstruct the individual charm and bottom meson decay vertices in these decays, and calculate the decay time for each B meson using the measured decay length and an estimate of the B meson energy. The resulting decay times are used to measure the B^0 and B^+ meson lifetimes. The results presented in this paper use OPAL data collected during the period 1991 to 1993, and thus update and replace our previous results [4].

2 The OPAL detector

A complete description of the OPAL detector may be found elsewhere [9, 10, 11]. We describe briefly the features of the detector pertinent to this analysis. Charged particle tracking is performed by the central detector which consists of a large volume jet chamber, a precision vertex drift chamber, a silicon microvertex detector and chambers which measure the z-coordinate[2] of tracks as they leave the jet chamber. Tracks in $Z^0 \to \mu^+\mu^-$ and $Z^0 \to e^+e^-$ events, with microvertex information, have an impact parameter resolution in r-ϕ of 16 μm. The microvertex detector reconstructs hits with an efficiency of 97% within the detector acceptance of $|\cos\theta| < 0.76$. The central detector is positioned inside a solenoid giving a uniform magnetic field of 0.435 T. The momentum resolution obtained is approximately $(\sigma_{p_{xy}}/p_{xy})^2 = (0.02)^2 + (0.0015 p_{xy})^2$, where p_{xy} is the momentum transverse to the beam direction in GeV. In addition to tracking charged particles, the jet chamber also provides measurements of ionisation energy loss dE/dx, which are used for particle identification. The solenoid is surrounded by a time-of-flight counter array and a lead-glass electromagnetic calorimeter with presampler. The instrumented return yoke of the magnet lies outside the electromagnetic calorimeter and forms the hadron calorimeter. This is surrounded by muon chambers.

[1] Most of the average b hadron lifetime measurements use inclusive semileptonic decays and therefore measure a mean weighted by relative production rates and semileptonic branching fractions.

[2] The OPAL coordinate system is defined by positive z along the electron beam direction, where θ and ϕ are the polar and azimuthal angles respectively.

Several simulated data samples have been used in this analysis. These were generated using the JETSET program [12, 13], passed through a simulation of the OPAL detector [14] and processed using the same reconstruction software as real data. To obtain larger samples, additional JETSET events have been processed using a faster simulation of the OPAL detector [14], which nevertheless describes the tracking detectors very well.

3 Particle identification

Charged pions and kaons are identified using $\mathrm{d}E/\mathrm{d}x$ information from the jet chamber [11]. The separation between pions and kaons is greater than two standard deviations for tracks of momentum between 2 and 20 GeV. We consider a particle to be consistent with a specific particle type if the probability for the measured $\mathrm{d}E/\mathrm{d}x$ value is greater than 1%. For kaons, if the measured $\mathrm{d}E/\mathrm{d}x$ lies between the expected kaon and pion values, we tighten this requirement to 3%.

The electron identification procedure used is similar to that described elsewhere [15] and uses $\mathrm{d}E/\mathrm{d}x$ information from the jet chamber and the quantity E_{cone}/p, where E_{cone} is the energy deposited in the electromagnetic calorimeter in a cone around the extrapolated position of the central detector track of momentum p. Electron candidates are selected by requiring the measured $\mathrm{d}E/\mathrm{d}x$ and E_{cone}/p to be not more than 2σ below the expected values for an electron. Candidates which are identified as photon conversions are rejected [16]. In addition the momentum of the electron must be greater than 2.0 GeV. The electron identification efficiency is about 80% in the kinematic range relevant to this analysis, for candidates within the acceptance $|\cos\theta| < 0.72$.

Muons are identified [16] by associating central detector tracks with track segments in the muon chambers. Loose requirements on $\mathrm{d}E/\mathrm{d}x$ are made to reject kaons and protons. The momentum of the muon candidate must be greater than 2.0 GeV. The average muon identification efficiency is approximately 75% for candidates within the acceptance $|\cos\theta| < 0.9$.

4 Event selection

This analysis is based on data recorded in 1991, 1992 and 1993 from $\mathrm{e^+e^-}$ annihilations at centre of mass energies between 88.5 and 93.8 GeV. The selection criteria for hadronic $\mathrm{Z^0}$ decays are described in a previous publication [17] and have an efficiency of $(98.4 \pm 0.4)\%$. After data quality and detector performance requirements, the available data sample consists of 1.72 million events.

4.1 Reconstruction of $\mathrm{B} \to \overline{\mathrm{D}}\ell^+\mathrm{X}$ and $\mathrm{B} \to \overline{\mathrm{D}}^*\ell^+\mathrm{X}$ decays

The selection criteria use both kinematic and vertex information from the decays, and remain similar to those used for our previous measurements [4]. Table 1 summarises the criteria for the four different decay modes.

$\overline{\mathrm{D}}^0$ and D^- mesons are selected by combining kaon and pion candidate tracks. In $\overline{\mathrm{D}}^0 \to \mathrm{K}^+\pi^-$ and $\mathrm{D}^- \to \mathrm{K}^+\pi^-\pi^-$ decays kaon candidates are required to have less than 5% probability of consistency with a pion hypothesis, to reduce the misidentification background. Pion candidates must have a momentum greater than 0.15 GeV. Kaon candidates must have a momentum exceeding 2.0 GeV, with the exception of candidates from the decay $\mathrm{D}^{*-} \longrightarrow \overline{\mathrm{D}}^0\pi^-, \overline{\mathrm{D}}^0 \longrightarrow$

Decay mode	p_{K} (GeV)	p_{π} (GeV)	$\mathrm{E_D}$ (GeV)	$\mid \cos\theta^* \mid$	$m_{\mathrm{D}^{(*)}\ell}$ (GeV)	$\mathrm{E}_{\mathrm{D}^{(*)}\ell}$ (GeV)	l_{D}/σ_l
$\mathrm{D}^- \to \mathrm{K}^+\pi^-\pi^-$	> 2	> 0.15	> 7	< 0.7	> 3.0	> 13.5	> 0
$\overline{\mathrm{D}}^0 \to \mathrm{K}^+\pi^-$	> 2	> 0.15	> 6	< 0.7	> 3.0	> 13.5	> -1
$\mathrm{D}^{*-} \to \overline{\mathrm{D}}^0\pi^-$, $\hookrightarrow \mathrm{K}^+\pi^-$	> 0.15	> 0.15	> 5	-	> 2.8	> 9.0	-
$\mathrm{D}^{*-} \to \overline{\mathrm{D}}^0\pi^-$, $\hookrightarrow \mathrm{K}^+\pi^-\pi^+\pi^-$	> 2	> 0.15	> 6	-	> 3.0	> 13.5	-

Table 1: Decay mode dependent selection criteria.

$\mathrm{K}^+\pi^-$ where the minimum momentum is reduced to 0.15 GeV because of the lower background within the sample.

D meson candidates must have an energy ($\mathrm{E_D}$) greater than 5–7 GeV, depending on the decay mode. For some decay modes we also cut on $\cos\theta^*$, where θ^* is the angle between the K^+ and the D boost direction in the D rest frame.

D^{*-} candidates are selected by combining a π^- with a $\overline{\mathrm{D}}^0$ candidate. The difference in mass between the D^{*-} and $\overline{\mathrm{D}}^0$ candidate must lie between 0.142–0.148 GeV. To ensure statistical independence and to obtain better separation of B^+ and B^0 mesons $\overline{\mathrm{D}}^0 \to \mathrm{K}^+\pi^-$ candidates are rejected if a $\mathrm{D}^{*-} \to \overline{\mathrm{D}}^0\pi^-$ candidate exists with a mass difference smaller than 0.16 GeV. This cut is also applied to both $(\mathrm{K}^+\pi^-)\pi^-$ combinations for the D^- candidates in order to reject D^{*-} mesons.

All combinations of leptons and D or D^* candidates within an event are considered as possible B candidates. To suppress random combinations the mass ($m_{\mathrm{D}^{(*)}\ell}$) and energy ($\mathrm{E}_{\mathrm{D}^{(*)}\ell}$) of the candidates must satisfy the minimum criteria shown in table 1. In addition all candidates must have $m_{\mathrm{D}^{(*)}\ell} < 5.35$ GeV.

The lepton track and at least two of the D decay tracks must be associated with at least one hit in the microvertex detector to ensure that vertex reconstruction is dominated by tracks with microvertex detector information. The association of microvertex hits to tracks found in the other central tracking detectors requires that the probability associated with the χ^2 be greater than 0.1% for all matches. Using a simulation of the OPAL detector [14] we find that particles leaving two (one) hits in the microvertex detector and resulting in a reconstructed track in the central detector have these hits correctly associated 96% (93%) of the time and are matched with one or more incorrect hits 2% (5%) of the time.

To reconstruct the B and D decay vertices the χ^2 of a vertex fit is minimised with respect to $(x_{\mathrm{B}}, y_{\mathrm{B}}, l_{\mathrm{D}}, \kappa_{i=1} \ldots \kappa_{i=n}, \phi_{i=1} \ldots \phi_{i=n})$ for a total of n tracks, where $(x_{\mathrm{B}}, y_{\mathrm{B}})$ are the coordinates of the B decay vertex, l_{D} is the decay length of the D meson and κ_i and ϕ_i are the curvature and angle of the i^{th} track at the relevant decay vertex. The direction of flight of the D meson is fixed to correspond to its momentum vector in the fit. We demand that the probability for

the vertex fit is greater than 1% in order to suppress random track combinations and badly reconstructed vertices. This requirement is tightened to 10% for the decay $D^- \longrightarrow K^+\pi^-\pi^-$ to reduce combinatorial background.

The B meson decay length is calculated in the r-ϕ plane using the reconstructed $\overline{D}^{(*)}\ell^+$ vertex position and the average e^+e^- interaction point [18]. It is signed according to the cosine of the angle between the vector separating (x_B, y_B) from the average interaction point and the $\overline{D}^{(*)}\ell^+$ momentum vector. To convert the decay length into three dimensions we estimate $\sin\theta$ for the B meson from the $\overline{D}^{(*)}\ell^+$ momentum vector. The B mesons have typical decay lengths of 3 mm which are reconstructed with a resolution of about 300 μm. We require that the error on the B decay length is less than 5 mm to reject a small fraction of poorly measured decays. The $\overline{D}^0$ (D^-) mesons have typical decay lengths of 1 mm (2.5 mm) with a typical decay length resolution of about 800 μm. As the reconstructed D decay length (l_D) is independent of the B decay length, and lifetime, it can be used to reject background. We require $|l_D| < 1$ cm for all decay modes. For the inclusive $\overline{D}^0$ (D^-) samples an additional cut on decay length significance is imposed ($l_D/\sigma_l > -1$ (0)), where σ_l is the calculated error on l_D.

4.2 Fitting the mass distributions

The resulting mass distributions for the four different decay modes are shown in figure 1. A clear signal is visible in each case. The two $K^+\pi^-$ mass distributions (figures 1b and 1c) also show a satellite peak around 1.6 GeV, which is expected from partially reconstructed decays, particularly $\overline{D}^0 \to K^+\rho^-, \rho^- \to \pi^-\pi^0$, in which the π^0 is not reconstructed. A similar enhancement is expected in the $K^+\pi^-\pi^-$ mass distribution (figure 1a). In the $D^{*-} \to \overline{D}^0\pi^-$ decay channel (figure 1c), the identification of a transition pion candidate ensures that the events contributing to this satellite peak originate almost entirely from D^{*-} decays. We are therefore able to use the events present in this satellite peak to provide additional statistics.

The signal and background in each channel are determined by fitting the mass distributions to a sum of Gaussians (to describe the signal and satellite peaks), and a second order polynomial background term. The resulting numbers of signal events for each channel are listed in table 2. The masses and widths of the Gaussians are allowed to vary in the fit, and the fitted values are consistent with those determined using a simulation of the corresponding processes in the OPAL detector [14]. Alternative parametrisations of both signal and background have been studied and produce little difference to the fitted number of background subtracted signal events.

4.3 Sources of background

B mesons which decay to $\overline{D}^{(*)}\ell^+$ through other incompletely reconstructed decay channels contribute to the background. Decays of the B_s to final states containing a $\overline{D}^{(*)}\ell^+$ combination, e.g. $B_s \to D_{s1}(2536)^-\ell^+\nu$, $D_{s1}(2536)^- \to D^{*-}\overline{K}^0$, are expected to form (2±1)% [19] of the event sample. These events are expected to have a small effect on the fitted lifetime unless the lifetime of the B_s differs significantly from those of the B^0 and B^+. Measurements of the B_s lifetime [6] indicate that it is close to the average b hadron lifetime. Although there are indications that the b baryon lifetime is lower [7] than the B^0 and B^+ lifetimes, it is not expected that b baryons will decay into $\overline{D}^{(*)}\ell^+$ final states. Combinations of $\overline{D}^{(*)}\ell^+$ may also result from B meson decays of the type $B \to D_s^{(*)+}\overline{D}^{(*)}, D_s^{(*)+} \to \ell^+X$, or $B \to \overline{D}^{(*)}\tau^+\nu X$ where the τ^+ decays to either an electron or a muon. Using $B(B \to D_s^{(*)+}\overline{D}^{(*)}) = 5.0 \pm 0.9\%$ [8] and

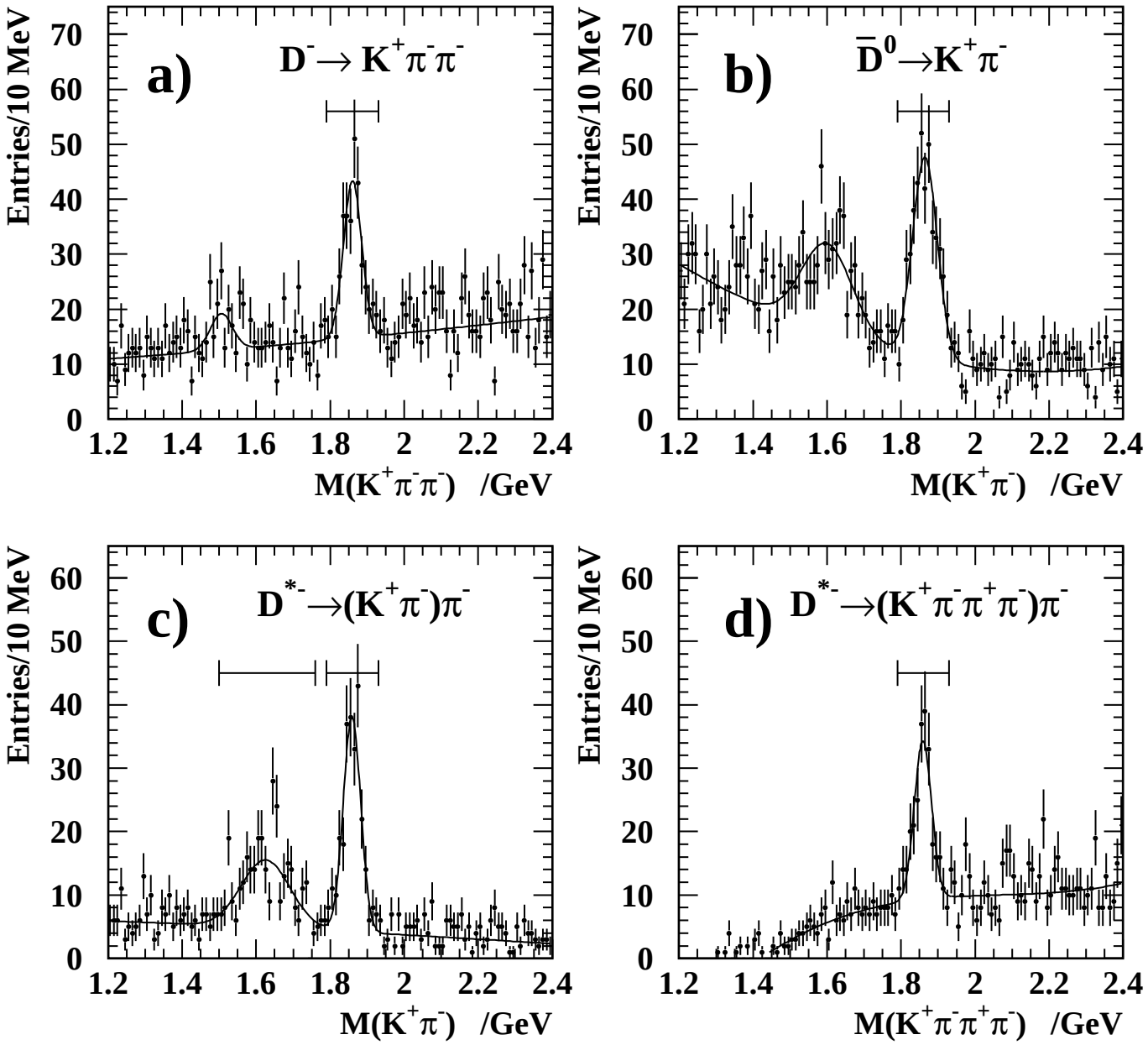

Figure 1: Mass distributions for; (a) $K^+\pi^-\pi^-$ combinations for events containing an ℓ^+; (b) $K^+\pi^-$ combinations for events containing an ℓ^+; (c) $K^+\pi^-$ combinations for events containing an ℓ^+; (d) $K^+\pi^-\pi^+\pi^-$ combinations for events containing an ℓ^+. Both (c) and (d) demand an additional pion for D^{*-} identification. The curves shown are the results of fits using Gaussians plus polynomial background functions. The indicated signal regions are within $\pm 3\sigma$ of the fitted D mass.

Decay mode	Signal
$D^- \to K^+\pi^-\pi^-$	170 ± 20
$\overline{D}^0 \to K^+\pi^-$	292 ± 23
$D^{*-} \to \overline{D}^0\pi^-$, $\overline{D}^0 \to K^+\pi^-$	198 ± 17
$D^{*-} \to \overline{D}^0\pi^-$, $\overline{D}^0 \to K^+\pi^-X$	174 ± 20
$D^{*-} \to \overline{D}^0\pi^-$, $\overline{D}^0 \to K^+\pi^-\pi^+\pi^-$	155 ± 17

Table 2: Number of background subtracted events for each decay mode.

$B(B \to \tau^+\nu X) = 3.3 \pm 0.8\%$ [20], we estimate that 0.6–1.5% of the $\overline{D}^{(*)}\ell^+$ event sample arises from the former source, and 1.0-1.6% from the latter. The effect of these events is examined as a source of systematic error (section 7).

The 'wrong sign' $\overline{D}^{(*)}\ell^-$ combinations provide a direct measure of the possible background of D mesons combined with fake leptons. No signals are observed in the $\overline{D}^{(*)}\ell^-$ combinations. We therefore conclude that the possible background from this source can be neglected.

5 Determination of the $\overline{D}^{(*)}\ell^+$ sample compositions

The B^0 and B^+ lifetimes can be determined once the probability of obtaining a B^0 (or B^+) meson for each event sample is known. In order to calculate this the relative amounts of B^0 and B^+ mesons decaying in each of the $\overline{D}^{(*)}\ell^+$ decay modes must first be found.

The different samples of $\overline{D}^{(*)}\ell^+$ events contain different fractions of B^0 and B^+ decays, due to the semileptonic decays of B^0 and B^+ mesons to pseudo-scalar, vector and P-wave charmed mesons. We use the symbol D^{**} to represent P-wave charmed mesons, possible non-resonant decays of the type $B \to \overline{D}(n\pi)\ell^+X$, and orbital and radial excitations. States containing $D^-\ell^+$ and $D^{*-}\ell^+$ would originate from B^0 in the absence of D^{**} production, as D^{*0} decays cannot produce D^-. B^+ can only decay to these states via D^{**}. Consequently the relative fraction of B^0 and B^+ mesons in the different $\overline{D}^{(*)}\ell^+$ samples depends on the relative production rate of the B mesons, their lifetimes (τ^0 and τ^+), the fractions (f^0, f^* and f^{**}) of semileptonic decays resulting in a D, D^* or D^{**} and the decay modes of the different D^* and D^{**} mesons.

We assume that the production rates of the B^0 and B^+ mesons in Z^0 decays are equal. This is expected because of isospin symmetry and the small mass difference between the states [8]. The sample compositions are found from the semileptonic branching ratios for B^0 or B^+ decaying to charm mesons. As the branching ratios can be expressed as the ratio of the partial to the total widths for B decay, and the total width is inversely proportional to lifetime, the sample compositions depend on the relative lifetimes. We assume that the partial widths for B^0 and B^+ decay are the same.

We assume that the D^{**} decays are dominated by the modes $D^{**} \to D^{(*)}\pi$ and use isospin

conservation to determine the relative fraction of the decays yielding charged and neutral $D^{(*)}$ mesons:

$$\begin{aligned} B(D^{**+} \to D^{(*)0}\pi^+) &= 2B(D^{**+} \to D^{(*)+}\pi^0), \\ B(D^{**0} \to D^{(*)+}\pi^-) &= 2B(D^{**0} \to D^{(*)0}\pi^0). \end{aligned} \tag{1}$$

We also parametrise the uncertainty in the relative production rates of pseudo-scalar and vector mesons in D^{**} decay by the quantity p_v:

$$p_v = \frac{B(D^{**} \to D^*X)}{B(D^{**} \to D^*X) + B(D^{**} \to DX)}. \tag{2}$$

We combine the predictions of the relative production rates from [21] with predictions [22] and measurements [8] of the branching ratios to obtain $p_v = 0.54$. A large variation of ± 0.3 is assigned to allow for all reasonable variations in the decay modelling. This value is consistent with the ARGUS [23] and LEP [19, 24] data which suggest that a significant fraction of the D^{**} states are the $J^P = 1^+$ and 2^+ states $D_1(2420)$ and $D_2^*(2460)$, respectively.

With these assumptions the relative fractions ($\mathcal{R}$) of B^0 and B^+ mesons in the different $\overline{D}^{(*)}\ell^+$ samples may be expressed as:

$$\begin{aligned} \mathcal{R}\left(\frac{B^0 \to \overline{D}^0\ell^+X}{B^+ \to \overline{D}^0\ell^+X}\right) &= \frac{\tau^0}{\tau^+}\left(\frac{(1-\eta^*)b^0 f^* + \frac{2}{3}f^{**} + \frac{1}{3}(1-\eta^*)b^0 p_v f^{**}}{f^0 + f^* + \frac{1}{3}f^{**} + \frac{2}{3}(1-\eta^*)b^0 p_v f^{**}}\right), \\ \mathcal{R}\left(\frac{B^0 \to D^-\ell^+X}{B^+ \to D^-\ell^+X}\right) &= \frac{\tau^0}{\tau^+}\left(\frac{f^0 + (1-b^0)f^* + \frac{1}{3}(1-p_v)f^{**} + \frac{1}{3}(1-b^0)p_v f^{**}}{\frac{2}{3}(1-b^0)p_v f^{**} + \frac{2}{3}(1-p_v)f^{**}}\right), \\ \mathcal{R}\left(\frac{B^0 \to D^{*-}\ell^+X}{B^+ \to D^{*-}\ell^+X}\right) &= \frac{\tau^0}{\tau^+}\left(\frac{f^* + \frac{1}{3}p_v f^{**}}{\frac{2}{3}p_v f^{**}}\right). \end{aligned} \tag{3}$$

Here b^0 is the branching ratio $B(D^{*+} \to D^0\pi^+)$, and η^* is the efficiency for removing a D^{*+} from the D^0 sample. We use the recent CLEO [25] measurement of $b^0 = 0.68 \pm 0.02$ and from our simulation determine η^* to be 0.96 ± 0.04.

In order to determine f^0, f^* and f^{**} we use measurements of the inclusive and exclusive semileptonic branching ratios of the B^0 or B^+ determined at the $\Upsilon(4S)$ centre-of-mass energy. The average exclusive branching ratios [8] for B decays to $D\ell^+\nu$ and $D^*\ell^+\nu$ are consistent for the B^0 and B^+. We therefore average over charged and neutral states and combine these numbers with the CLEO [26] measurement of $f^{**} = 0.36 \pm 0.12$ to obtain:

$$\begin{aligned} f^0 &= \frac{B(B \to \overline{D}\ell^+\nu)}{B(B \to \overline{D}\ell^+\nu) + B(B \to \overline{D}^*\ell^+\nu)}(1 - f^{**}) = 0.18, \\ f^* &= \frac{B(B \to \overline{D}^*\ell^+\nu)}{B(B \to \overline{D}\ell^+\nu) + B(B \to \overline{D}^*\ell^+\nu)}(1 - f^{**}) = 0.46. \end{aligned}$$

We also calculate the reconstruction efficiencies for $B \to \overline{D}^*\ell^+\nu$ decays and $B \to \overline{D}^{**}\ell^+\nu$ decays relative to $B \to \overline{D}\ell^+\nu$ from our simulation. We find these to be in the range 0.93–0.96 for the former case, and between 0.80–0.93 for the latter, and include these in the calculation. Assuming that the B^0 and B^+ lifetimes are equal, we find that B^0 mesons form 72% of the $D^-\ell^+$, 25% of the $\overline{D}^0\ell^+$ and 79% of the $D^{*-}\ell^+$ event samples.

6 Lifetime fitting

In order to estimate a decay time for these events we first develop a method to reconstruct the B meson energy. We then fit the resulting decay time distributions using a maximum likelihood method to extract the lifetimes of the different $\overline{\mathrm{D}}^{(*)}\ell^+\nu$ event samples. Finally, in section 6.3, we extend the method to fit for the B^0 and B^+ meson lifetimes.

6.1 Energy reconstruction

In the semileptonic decay $\mathrm{B} \to \overline{\mathrm{D}}^{(*)}\ell^+\nu$, the energy reconstructed ($\mathrm{E}_{\mathrm{D}^{(*)}\ell}$) from the B decay products is lower than the parent energy (E_{B}) because of the undetected neutrino. Applying two body decay kinematics, the observable $\mathrm{E}_{\mathrm{D}^{(*)}\ell}$ is given in the laboratory frame by

$$\mathrm{E}_{\mathrm{D}^{(*)}\ell} = \frac{\mathrm{E}_{\mathrm{B}}}{2m_{\mathrm{B}}^2}\{m_{\mathrm{B}}^2 + m_{\mathrm{D}^{(*)}\ell}^2 + \beta_{\mathrm{B}}(m_{\mathrm{B}}^2 - m_{\mathrm{D}^{(*)}\ell}^2)\cos\theta_{\mathrm{B}}^*\} \tag{4}$$

where θ_{B}^* is the angle of the $\overline{\mathrm{D}}^{(*)}\ell^+$ flight direction to the boost vector in the B rest frame, and β_{B} is $(\sqrt{\mathrm{E}_{\mathrm{B}}^2 - m_{\mathrm{B}}^2})/\mathrm{E}_{\mathrm{B}}$.

Given values of $\mathrm{E}_{\mathrm{D}^{(*)}\ell}$ can arise from a range of E_{B} as $\cos\theta_{\mathrm{B}}^*$ varies. The distribution in $\cos\theta_{\mathrm{B}}^*$ is flat (because the B meson is a pseudoscalar particle), and the probability of each E_{B} is governed by the underlying fragmentation function.

We define the probability function $\mathrm{P}(\mathrm{E}_B \mid \mathrm{E}_{\mathrm{D}^{(*)}\ell}, m_{\mathrm{D}^{(*)}\ell})$ as the probability of obtaining each possible E_{B}, given the experimental inputs $\mathrm{E}_{\mathrm{D}^{(*)}\ell}$ and $m_{\mathrm{D}^{(*)}\ell}$. Using Bayes' theorem [27], we express this in the form;

$$\mathrm{P}(\mathrm{E}_B \mid \mathrm{E}_{\mathrm{D}^{(*)}\ell}, m_{\mathrm{D}^{(*)}\ell}) = \frac{\mathrm{P}(\mathrm{E}_{\mathrm{D}^{(*)}\ell} \mid \mathrm{E}_B, \mathrm{m}_{\mathrm{D}^{(*)}\ell})\mathrm{P}(\mathrm{E}_B)}{\int_{\mathrm{E}_{\mathrm{min}}}^{\mathrm{E}_{\mathrm{max}}} \mathrm{P}(\mathrm{E}_{\mathrm{D}^{(*)}\ell} \mid \mathrm{E}, \mathrm{m}_{\mathrm{D}^{(*)}\ell})\mathrm{P}(\mathrm{E})d\mathrm{E}} \tag{5}$$

where $\mathrm{P}(\mathrm{E}_{\mathrm{D}^{(*)}\ell} \mid \mathrm{E}_B, m_{\mathrm{D}^{(*)}\ell})$ follows from equation 4, and $\mathrm{P}(\mathrm{E}_B)$ is an estimate of the b fragmentation spectrum. We use a Peterson fragmentation function [28] with $\epsilon = 0.055$ as an estimate of the b fragmentation function in equation 5, although the result is only weakly dependent on this choice. $\mathrm{E_{min}}$ and $\mathrm{E_{max}}$ are the minimum and maximum E_{B} (equal to the lowest kinematic cut for $\mathrm{E}_{\mathrm{D}^{(*)}\ell}$ and the beam energy respectively) used in the calculation. In this way only physical energies are considered. Note that as E_{B} is independent of $m_{\mathrm{D}^{(*)}\ell}$, no probability distributions for $m_{\mathrm{D}^{(*)}\ell}$ appear in equation 5.

Figure 2 shows the agreement obtained between the true B energies and the output of the method on a sample of approximately 7 000 fast simulation events [14] for the decay mode $\mathrm{B} \longrightarrow \overline{\mathrm{D}}^0\ell^+\nu, \overline{\mathrm{D}}^0 \longrightarrow \mathrm{K}^+\pi^-$.

6.2 Fitting for the average lifetime

We use an unbinned maximum likelihood fit to extract the B meson lifetimes from data. The lifetime fit uses events which lie within $\pm 3\sigma$ of the fitted D mass for each decay mode. This requirement is tightened to $\pm 2\sigma$ for events from the sample $\mathrm{D}^{*-} \to (\mathrm{K}^+\pi^-\mathrm{X})\pi^-$, in order to minimise background in this channel and avoid overlap with events from the fully reconstructed $\mathrm{D}^{*-} \to (\mathrm{K}^+\pi^-)\pi^-$ sample.

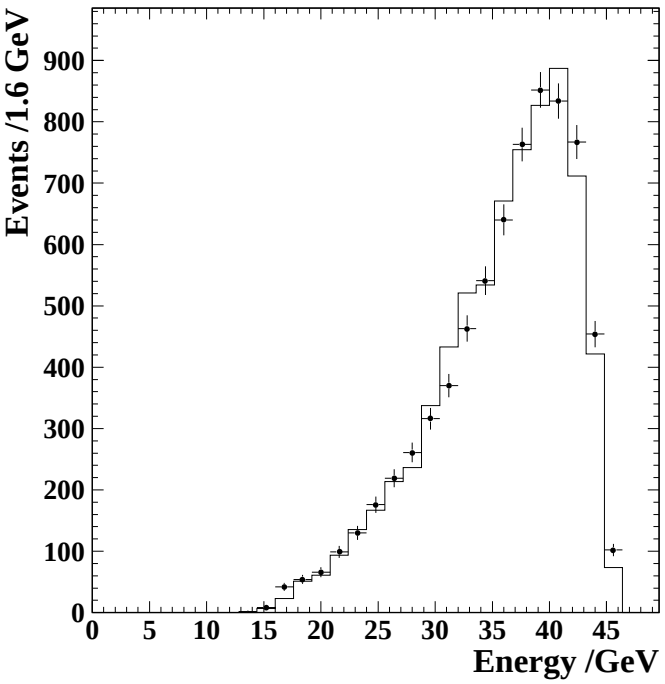

Figure 2: Output of the probabilistic energy correction scheme for simulated $\mathrm{B} \longrightarrow \overline{\mathrm{D}}^0 \ell^+ \nu, \overline{\mathrm{D}}^0 \longrightarrow \mathrm{K}^+\pi^-$ decays. The points are the true parent B energy and the solid histogram the output from the method.

The likelihood function for the background decay times, $\mathcal{L}_{back}$, is parameterised using a function of the form

$$\mathcal{L}_{back}(l; c_1, c_2, c_3, c_4, c_5) = c_1 \cdot c_2 \cdot \mathcal{E}(l; \sigma_l, c_3) + c_1 \cdot (1 - c_2) \cdot \mathcal{E}(l; \sigma_l, -c_5) + (1 - c_1) \cdot \mathcal{G}(l; c_4 \cdot \sigma_l) \quad (6)$$

where

$$\mathcal{E}(l; \sigma_l, \mu) = \mathrm{N} \int_{\mathrm{E_{min}}}^{\mathrm{E_{max}}} \mathrm{P}(E \mid \mathrm{E}_{\mathrm{D}^{(*)}\ell}, m_{\mathrm{D}^{(*)}\ell}) \left[\int_0^{+\infty} \frac{1}{\beta \mathrm{E}} e^{-(l' m_B)/(\beta c E \mu)} e^{-0.5(\frac{l-l'}{\sigma_l})^2} \mathrm{d}l' \right] \mathrm{d}E$$

and

$$\mathcal{G}(l; \sigma_l) = \mathrm{N}' \int_{\mathrm{E_{min}}}^{\mathrm{E_{max}}} \mathrm{P}(E \mid \mathrm{E}_{\mathrm{D}^{(*)}\ell}, m_{\mathrm{D}^{(*)}\ell}) [e^{-0.5(\frac{l}{\sigma_l})^2}] \mathrm{d}E$$

Here $\mathrm{P}(E \mid \mathrm{E}_{\mathrm{D}^{(*)}\ell}, m_{\mathrm{D}^{(*)}\ell})$ is the associated probability for the value of E in the integrand. $\mathcal{G}(l; \sigma_l)$ denotes a Gaussian of width σ_l centred at zero, and $\mathcal{E}(l; \sigma_l, \mu)$ an exponential of mean μ convolved with a Gaussian of width σ_l and mean zero. The quantity σ_l is the decay length error for each event, and $\beta = (\sqrt{E^2 - m_{\mathrm{B}}^2})/E$ for each value of E in the integrand. N and N$'$ are normalising factors such that the integrated probability over all decay lengths is 1.

The positive and negative going exponential terms in $\mathcal{L}_{back}$ are intended to describe the fraction of background arising from b events and which have residual lifetime. Background arising from u,d,s and c events is parametrised by a Gaussian of variable width. The parameters c_1, c_2, c_3, c_4 and c_5 are determined separately for each of the decay modes. Typical values for c_3, for example, vary between 1.0 and 2.5 ps, whereas c_5 varies between 0.0 and 2.2 ps.

Decay mode	Fit result (ps)
$D^- \to K^+\pi^-\pi^-$	$1.30^{+0.15}_{-0.14}$
$\overline{D}^0 \to K^+\pi^-$	$1.53^{+0.12}_{-0.11}$
$D^{*-} \to \overline{D}^0\pi^-$, $\overline{D}^0 \to K^+\pi^-$	$1.65^{+0.16}_{-0.14}$
$D^{*-} \to \overline{D}^0\pi^-$, $\overline{D}^0 \to K^+\pi^-X$	$1.81^{+0.24}_{-0.27}$
$D^{*-} \to \overline{D}^0\pi^-$, $\overline{D}^0 \to K^+\pi^-\pi^+\pi^-$	$1.46^{+0.18}_{-0.17}$
Combined sample	1.53 ± 0.07

Table 3: Lifetime fit results for the different $\overline{D}^{(*)}\ell^+$ samples. Errors are statistical only.

The signal likelihood function, $\mathcal{L}_{sig}$, is given by

$$\mathcal{L}_{sig}(l;\tau) = \mathcal{E}(l;\sigma_l,\tau) \tag{7}$$

where τ is the fitted mean lifetime. We fit both signal and background simultaneously using a likelihood function of the form

$$\mathcal{L}(l;\tau,c_1,c_2,c_3,c_4,c_5) = \prod_i \left(f_i \cdot \mathcal{L}_{sig}(l;\tau) + (1-f_i)\cdot \mathcal{L}_{back}(l;c_1,c_2,c_3,c_4,c_5)\right) \tag{8}$$

where f_i is the probability that a particular event i is signal. This is determined using the measured D mass for each event and the fit results to the mass region outlined in section 4.

Table 3 lists the fitted lifetimes found for each decay channel with their statistical errors, together with the average lifetime of the combined sample. The results are consistent with this average and show a reasonable spread. The fits themselves are illustrated in figure 3.

6.3 Fitting the B^0 and B^+ lifetimes

The B^0 and B^+ compositions of the $\overline{D}^{(*)}\ell^+$ event samples have been determined in section 5. We now use the combined sample of $\overline{D}^{(*)}\ell^+$ events to fit τ^0 and τ^+, as well as directly fitting the lifetime ratio τ^+/τ^0. The likelihood function ($\mathcal{L}$) given in equation 8 is modified to include two signal terms of different lifetimes. The relative weight of both is determined by the assigned probability of a particular event being B^0 or B^+.

As neutral decay particles such as γ or π^0 are not reconstructed in D^{**} and some D^* decays, the energy (and thus lifetime) estimate is low. Lifetime bias correction factors (ranging between -0.6% and 2.3%) are calculated from our simulation and applied to B^0 and B^+ separately within the fit for each decay mode, as the probability of D, D^* and D^{**} production varies with the decay channel under consideration.

The fit results and statistical errors are:

$$\tau^0 \;=\; 1.53 \pm 0.12 \;\; \text{ps},$$

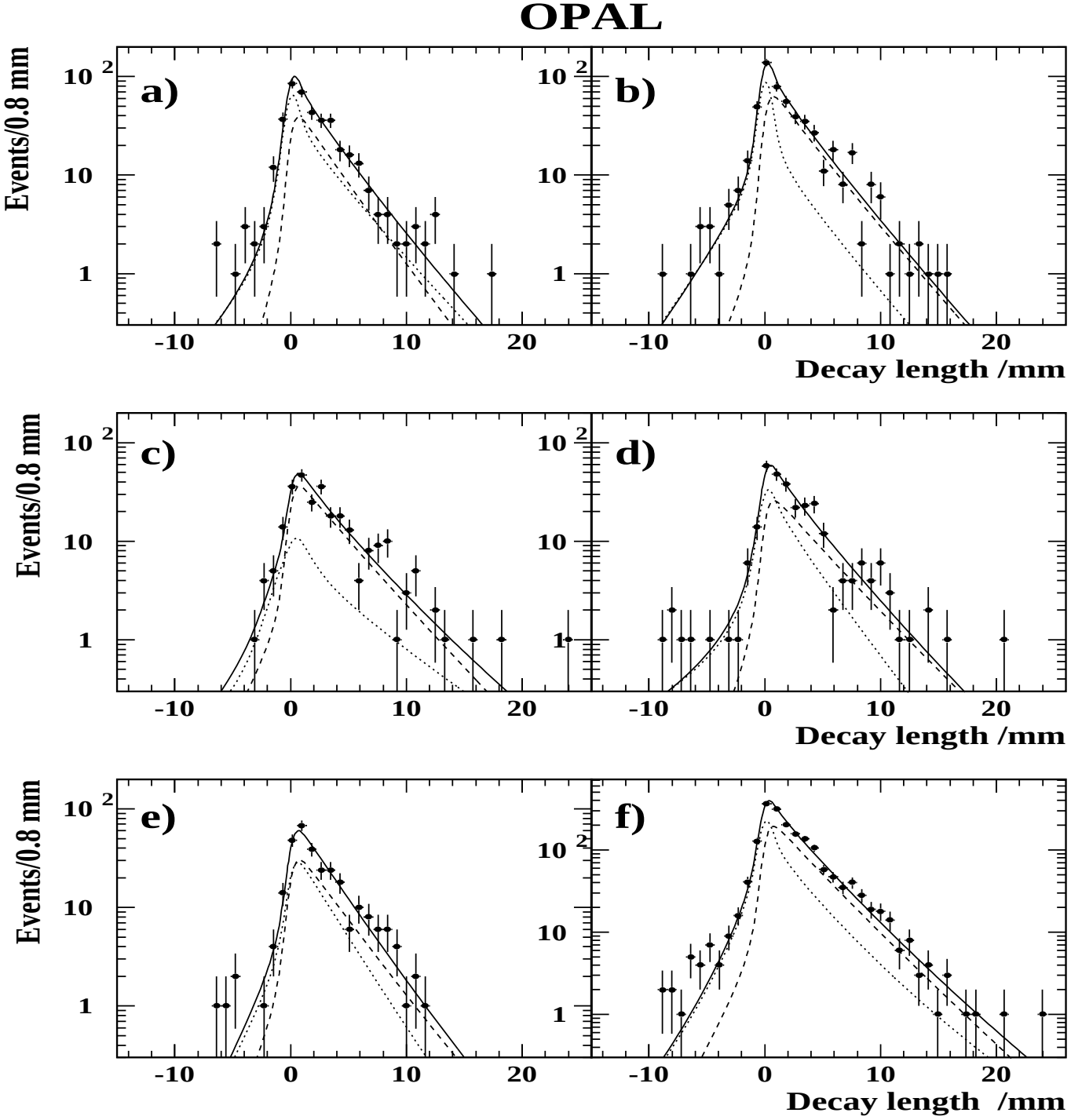

Figure 3: Decay length distributions for; a) $D^- \to K^+\pi^-\pi^-$ events; b) $\overline{D}^0 \to K^+\pi^-$ events; c) $D^{*-} \to \overline{D}^0\pi^-$, $\overline{D}^0 \to K^+\pi^-$ events; d) $D^{*-} \to \overline{D}^0\pi^-$, $\overline{D}^0 \to K^+\pi^-X$ events; e) $D^{*-} \to \overline{D}^0\pi^-$, $\overline{D}^0 \to K^+\pi^-\pi^+\pi^-$ events; f) all modes together within a region $\pm 3\sigma$ from the fitted D mass. In all cases the points are the measured decay lengths for the events used in the fit. The dashed curve represents the contribution to the fit due to signal, and the dotted curve that due to background. The solid curve illustrates the combined fit result to signal and background.

Measurement	$\pm 2\sigma$ region	$\pm 3\sigma$ region	$\pm 4\sigma$ region
τ^0	1.59 ± 0.12 ps	1.53 ± 0.12 ps	1.56 ± 0.12 ps
τ^+	1.59 ± 0.15 ps	1.52 ± 0.14 ps	1.58 ± 0.14 ps
τ^+/τ^0	1.00 ± 0.14	0.99 ± 0.14	1.01 ± 0.14
$\langle\tau\rangle$	1.59 ± 0.07 ps	1.53 ± 0.07 ps	1.56 ± 0.07 ps

Table 4: Lifetime fit results for the different fit regions tested. The errors quoted are statistical.

$$\tau^+ = 1.52 \pm 0.14 \text{ ps},$$

$$\tau^+/\tau^0 = 0.99 \pm 0.14.$$

7 Systematic uncertainties

The systematic uncertainties in the fitting procedure arise from four sources: the treatment of the background; the fitting method; detector effects; and the uncertainty in the B^0 and B^+ content of each event sample. These are summarised in table 5.

7.1 The background

The treatment of the background contains three sources of systematic error. The first is due to the estimated shape of the decay time distribution. Different parametrisations of this distribution have been tested. Signal terms (equation 7) of fixed B^0, B^+ or B_s lifetime [8] have also been added to the background likelihood to investigate the effects on the fitted lifetimes of the expected number of background events listed in section 4. The largest deviation noted in both tests was taken as the systematic error. Another source of error arises from the statistical precision of the fit to the D mass distributions, which gives an error on the signal probability in the lifetime fit. This error was determined by taking 100 sets of mass fit coefficients that are normally distributed (according to both errors and correlations) about their nominal values. The standard deviations obtained by varying the signal probabilities for each channel in turn and refitting the lifetimes were added in quadrature to give the systematic error. A final source of error arises from the fit region used to determine the lifetimes. We quote an error equal to the largest deviation observed when repeating the analysis using events from $\pm 2\sigma$ and $\pm 4\sigma$ of the fitted D mass (see table 4). It should be noted that the lifetime ratio remains constant and that τ^0 and τ^+ are statistically consistent.

7.2 The fitting method

The fitting method also contains three sources of systematic error. The first is due to our estimate of $P(E_B)$. We vary ϵ, the Peterson fragmentation function parameter, between the limits 0.0025 and 0.0095 [29] and redetermine the lifetimes at these values. The difference between

the refitted and standard lifetimes is taken as the systematic error. Other estimates, including a flat function, have been applied to simulated event samples as an additional check. The largest deviation observed (0.6%) is smaller than the systematic error quoted. The experimental inputs $E_{D^{(*)}\ell}$ and $m_{D^{(*)}\ell}$ contain two further sources of error due to finite detector resolution and D^{**} production, where neutral decay products such as γ or π^0 are not reconstructed. A correction factor for the bias introduced by this latter source ($1.3 \pm 1.2\%$) and errors for both were calculated using our simulation. The latter effect is included within the fit.

7.3 Detector effects

We have considered the influence of detector effects on the fitted lifetimes. The decay length and therefore the lifetime of each B candidate will be affected by any misalignment of the silicon detector. In our previous study [4] we found that coherent radial shifts of $\pm 50\mu$m corresponded to a decay length uncertainty of 35 μm, which translates to an error on the lifetime of 0.02 ps. Movements of the interaction point of $\pm 25\mu$m in x- and y-directions have been studied using simulated events, and the effect on the lifetimes noted. The decay length error σ_l has also been varied by $\pm 20\%$ to cover both charged track extrapolation and silicon hit resolution uncertainties in order to determine this source of systematic error.

We have also studied the effect on the fit of multiplying the decay length errors by a scale factor. To avoid correlation between this scale factor and the background coefficients the lifetime fits were performed in two stages. The background coefficients in each decay mode sample were first fitted using events from a higher mass sideband region (2.0 to 2.2 GeV). The form of the background likelihood was then fixed with these coefficients, and events from the fit region fitted to determine the average lifetime and the scale factor. The scale factor was found to be 1.04 ± 0.11, indicating that the tracking errors are well understood.

7.4 The B^0 and B^+ content of each sample

The last source of systematic errors is from an uncertainty in sample composition. To evaluate this we allow the dominant uncertainties (due to p_v and f^{**}) to vary by $\pm\sigma$. As the probability calculation is proportional to the ratio of lifetimes τ^+/τ^0, we refit the lifetimes where the probabilities are calculated at values of $\tau^+/\tau^0 \pm \sigma$. The deviation between these refitted lifetimes and the standard values are taken as the systematic error due to this source.

Source	τ^0	τ^+	τ^+/τ^0	$\langle\tau\rangle$
Background decay time shape	±0.01	±0.02	±0.02	±0.01
Signal probability	±0.02	±0.02	±0.02	±0.01
Fit region	±0.06	±0.07	±0.02	±0.06
$p(E_B)$ estimator	$^{+0.01}_{-0.02}$	$^{+0.01}_{-0.02}$	-	$^{+0.01}_{-0.02}$
$E_{D^{(*)}\ell}$, $m_{D^{(*)}\ell}$ resolution	±0.01	±0.01	-	±0.01
Incomplete reconstruction	±0.02	±0.02	-	±0.02
Microvertex alignment	±0.02	±0.02	-	±0.02
Interaction point	±0.01	±0.01	-	±0.01
σ_l	$^{+0.02}_{-0.03}$	±0.02	-	±0.02
Probability inputs	$^{+0.02}_{-0.01}$	$^{+0.02}_{-0.03}$	$^{+0.03}_{-0.02}$	-
$\tau^+/\tau^0 \pm \sigma$	±0.01	±0.01	±0.01	-
Total	±0.08	±0.09	$^{+0.05}_{-0.04}$	±0.07

Table 5: Summary of systematic errors for each measurement. All values other than those for the ratio are in picoseconds. Errors are combined in quadrature.

8 Conclusions

We have used a sample of approximately 1000 $B \to \overline{D}\ell^+X$ and $B \to \overline{D}^*\ell^+X$ events to measure the B^0 and B^+ meson lifetimes directly, with the results;

$$\tau^0 = 1.53 \pm 0.12 \pm 0.08 \text{ ps},$$

$$\tau^+ = 1.52 \pm 0.14 \pm 0.09 \text{ ps},$$

$$\tau^+/\tau^0 = 0.99 \pm 0.14^{+0.05}_{-0.04}$$

These results support expectations that the lifetimes are similar. The average B lifetime for the mixture of B mesons in this event sample is $\langle\tau\rangle = 1.53 \pm 0.07 \pm 0.07$ ps. These measurements supersede our previous results [4], which were obtained using a subset of this data sample.

9 Acknowledgements

It is a pleasure to thank the SL Division for the efficient operation of the LEP accelerator, the precise information on the absolute energy, and their continuing close cooperation with our experimental group. In addition to the support staff at our own institutions we are pleased to acknowledge the
Department of Energy, USA,
National Science Foundation, USA,
Particle Physics and Astronomy Research Council, UK,
Natural Sciences and Engineering Research Council, Canada,
Fussefeld Foundation,
Israel Ministry of Science,
Israel Science Foundation, administered by the Israel Academy of Science and Humanities,
Minerva Gesellschaft,
Japanese Ministry of Education, Science and Culture (the Monbusho) and a grant under the Monbusho International Science Research Program,
German Israeli Bi-national Science Foundation (GIF),
Direction des Sciences de la Matière du Commissariat à l'Energie Atomique, France,
Bundesministerium für Forschung und Technologie, Germany,
National Research Council of Canada,
A.P. Sloan Foundation and Junta Nacional de Investigação Científica e Tecnológica, Portugal.

References

[1] See for example:
I. I. Bigi, *Phys. Lett.* **B169** (1986) 1;
J. H. Kühn *et al.*, in 'Z physics at LEP 1', *CERN 89-08* (1989) ed. G. Altarelli *et al.*;
G. Altarelli and S. Petrarca, *Phys. Lett.* **B261** (1991) 303;
I. I. Bigi and N. G. Uraltsev, *Phys. Lett.* **B280** (1992) 271.

[2] Average B lifetime measurements from Z^0 decays:
ALEPH Collaboration, D. Buskulic *et al.*, *Phys.Lett.* **B314** (1993) 459;
DELPHI Collaboration, P. Abreu *et al.*, *Z. Phys.* **C63** (1994) 3;
L3 Collaboration, O. Adriani *et al.*, *Phys. Lett.* **B317** (1993) 474;
OPAL Collaboration, P. D. Acton *et al.*, *Z. Phys.* **C60** (1993) 217.

[3] CLEO Collaboration, B. Barish *et al*, *CLNS-94-1285* (1994)

[4] OPAL Collaboration, P. D. Acton *et al*, *Phys. Lett.* **B307** (1993) 247;

[5] B^0 and B^+ meson lifetime measurements:
ALEPH Collaboration, D. Buskulic *et al.*, *Phys. Lett.* **B307** (1993) 194;
DELPHI Collaboration, P. Abreu *et al.*, *Z. Phys.* **C57** (1993) 181;
DELPHI Collaboration, P. Abreu *et al.*, *Phys. Lett.* **B312** (1993) 253;
CDF Collaboration, F. Abe *et al.*, *Phys. Rev. Lett.* **72** (1994) 3456.

[6] B_s meson lifetime measurements :
ALEPH Collaboration, D. Buskulic *et al.*, *Phys. Lett.* **B322** (1994) 275;
DELPHI Collaboration, P. Abreu *et al.*, *Z. Phys.* **C61** (1994) 407;
OPAL Collaboration, P. D. Acton *et al.*, *Phys. Lett.* **B312** (1993) 501;
OPAL Collaboration, R. Akers *et al.*, *CERN-PPE/95-20* (1995);
CDF Collaboration, F. Abe *et al.*, *FERMILAB-PUB-94-420-E* (1995).

[7] b baryon lifetime measurements:
DELPHI Collaboration, P. Abreu *et al.*, *Phys. Lett.* **B311** (1993) 379;
OPAL Collaboration, R. Akers *et al.*, *Phys. Lett.* **B316** (1993) 435;
ALEPH Collaboration, D. Buskulic *et al.*, *Phys. Lett.* **B297** (1992) 449.

[8] Particle Data Group, L. Montanet *et al.*, *Phys. Rev.* **D50** (1994) 1173.

[9] OPAL Collaboration, K. Ahmet *et al.*, *Nucl. Instrum. Methods* **A305** (1991) 275.

[10] P. P. Allport *et al.*, *Nucl. Instrum. Methods* **A324** (1993) 34,
P. P. Allport *et al.*, *Nucl. Instrum. Methods* **A346**(1994) 476.

[11] M. Hauschild *et al.*, *Nucl. Instrum. Methods* **A314** (1992) 74.

[12] T. Sjöstrand, *Comp. Phys. Comm.* **39** (1986) 347.

[13] OPAL Collaboration, M. Z. Akrawy *et al.*, *Z. Phys.* **C47** (1990) 505.

[14] J. Allison *et al.*, *Nucl. Instrum. Methods* **A317** (1992) 47.

[15] OPAL Collaboration, R. Akers *et al.*, *Z. Phys.* **C60**(1993) 199.

[16] OPAL Collaboration, R. Akers *et al. Z. Phys.* **C65** (1995) 17.

[17] OPAL Collaboration, G. Alexander *et al.*, *Z. Phys.* **C52** (1991) 175.

[18] OPAL Collaboration, P. D. Acton *et al. Z. Phys.* **C59** (1993) 183;
OPAL Collaboration, R. Akers *et al. Phys. Lett.* **B338** (1994) 497.

[19] OPAL Collaboration, R. Akers *et al. CERN-PPE/95-02* (1995).

[20] ALEPH Collaboration, D. Buskulic *et al.*, *Phys. Lett.* **B298** (1993) 479;
L3 Collaboration, M. Acciarri *et al.*, *Phys. Lett.* **B332** (1994) 201.

[21] P. Colangelo, G. Nardulli and N. Paver, *Phys. Lett.* **B293** (1992) 207.

[22] J. L. Rosner, *Comm. Nucl. Part. Phys.* (1986) 109;
S. Godfrey and R. Kokoski, *Phys. Rev.* **D43** (1991) 1679.

[23] ARGUS Collaboration, H. Albrecht *et al.*, *Z. Phys.* **C57** (1993) 533.

[24] ALEPH Collaboration, D. Buskulic *et al. Phys. Lett.* **B345** (1995) 103.

[25] CLEO Collaboration, F. Butler *et al.*, *Phys. Rev. Lett.* **69** (1992) 2041.

[26] CLEO Collaboration, R. Fulton *et al.*, *Phys. Rev.* **D43** (1991) 651.

[27] See, for example:
R. J. Barlow 'Statistics: a guide to the use of statistical methods in the Physical Sciences' John Wiley and sons.

[28] C. Peterson, D. Schlatter, I. Schmitt and P. M. Zerwas, *Phys. Rev.* **D27** (1983) 105.

[29] OPAL Collaboration, P. D. Acton *et al. Z. Phys.* **C60** (1993) 217.